Moon Eunseong (Orcid ID: 0000-0003-3378-7930)

High-Efficiency Photovoltaic Modules on a Chip for Millimeter-Scale Energy Harvesting

Eunseong Moon, Inhee Lee, David Blaauw and Jamie D. Phillips
Department of Electrical Engineering and Computer Science
University of Michigan, Ann Arbor, Michigan, USA

Abstract

Photovoltaic modules at the mm-scale are demonstrated in this work to power wirelessly interconnected mm-scale sensor systems operating under low flux conditions, enabling applications in the Internet of Things and biological sensors. Module efficiency is found to be limited by perimeter recombination for individual cells, and shunt leakage for the series-connected module configuration. We utilize GaAs and AlGaAs junction barrier isolation between interconnected cells to dramatically reduce shunt leakage current. A photovoltaic module with eight series-connected cells and total area of 1.27-mm^2 demonstrates a power conversion efficiency of greater than 26 % under low-flux near infrared illumination (850 nm at 1 µW/mm^2). The output voltage of the module is greater than 5 V, providing a voltage up-conversion efficiency of more than 90 %. We demonstrate direct photovoltaic charging of a 16 µAh pair of thin-film lithium-ion batteries under dim light conditions, enabling the perpetual operation of practical mm-scale wirelessly interconnected systems.

Key words: Monolithic photovoltaic module, Millimeter-scale energy harvesting, Internet of Things, Gallium arsenide, Photo-induced shunt, Perimeter recombination

1. Introduction

Continued scaling of electronic systems, and the proliferation of wireless sensor networks that have enabled the Internet of Things (IoT) [1-3], necessitate a means of energy harvesting to achieve self-powered devices with small form factors. Photovoltaics (PV) are well known for efficient large scale power generation and for their use in self-powered electronic devices at the macroscale. While the physical dimensions of PV devices and systems may be reduced, miniaturization to the mm-scale present new challenges in achieving high conversion efficiency. Furthermore, sources such as ambient indoor lighting or infrared radiation for wireless power transfer differ dramatically from solar irradiance in terms of both spectral content and flux [4-7]. Dark current and shunt conductive paths in photovoltaic cells become much more important at small dimensions and low flux ambient indoor conditions [4-9] in comparison to typical outdoor

solar irradiation (approximately a factor of 1,000 lower flux than AM 1.5). High-efficiency PV cells can meet the power requirements (> 50 nW/mm^2) of these systems through optimization of the spectral response in appropriate spectral windows: 425-650 nm for ambient indoor lighting [4] and 700-1100 nm for the infrared transparency window for biological tissue [3]. GaAs-based PV cells can provide outstanding performance in these desired wavelength regions due to a large shunt resistance and range of tunable bandgap energies (larger bandgap at 1.67 eV from $Al_{0.2}Ga_{0.8}As$ for indoor lighting [10] and smaller bandgap at 1.424 eV from GaAs for infrared illumination [5]) to maximize power conversion efficiency. Previously, power conversion efficiency values above 20 % under white room lighting at 580 lux (1.24 μW/mm^2) [10] and above 30 % under 850 nm infrared LED illumination at 1 μW/mm^2 [5] were achieved using single-junction GaAs cells.

The most critical issue in ensuring perpetual operation of systems is the overall power generation. In contrast to large-area applications, cost per unit area is a secondary factor in mm-scale systems due to the small PV area (and hence, low cost). This enables the use of high-performance materials such as III-V compound semiconductors. Furthermore, to maximize energy capacity, the battery of the mm-scale systems often have a high open-circuit voltage, which is several times higher than the typical open circuit voltage of a single photovoltaic cell [11]. A switched capacitor network is typically used to achieve voltage up-conversion, where switching and resistive losses limit efficiency to approximately 50 % [12]. Direct series/parallel connections of PV cells provide an appealing alternative for voltage up-conversion, where a PV network with over 80 % power conversion efficiency has been demonstrated [12]. However, monolithic PV arrays present several challenges in minimizing losses associated to device isolation and shunt leakage paths between series connections [9,13]. Monolithic silicon PV arrays present several challenges including low voltage generation (large number of series-connected cells required to achieve desired voltage) and low optical absorption strength (thick absorber regions are required, making device isolation problematic) [9,11,14]. The larger voltage generation and high optical absorption strength of GaAs and related compound semiconductors provide a much more attractive platform for monolithic PV modules. Previously, a laser power converter based on a six-cell GaAs PV module array was demonstrated at the mm-scale with conversion efficiency greater than 52 % under monochromatic illumination at 13.2 W/cm^2 (132 mW/mm^2), with efficiency limited by perimeter recombination and shunt leakage through the semi-insulating GaAs substrate [9]. In this work, we present monolithic GaAs-based PV modules at the mm-scale operating under low flux conditions (<10 μW/mm^2) as a means to power IoT systems or bio-implantable sensors without the requirement for DC-DC voltage up-conversion.

2. Experiment

We used a baseline PV cell structure (Fig. 1 a) grown by molecular beam epitaxy (MBE) based on our previously reported high-efficiency single-junction GaAs PV cells [5], where the critical

limiting factor from exposed sidewall/perimeter recombination losses of single PV cells was dramatically reduced utilizing the ammonium sulfide chemical treatment and subsequent silicon nitride deposition. Monolithic PV arrays were constructed on semi-insulating GaAs substrates. While the semi-insulating GaAs substrate provides a high-resistivity material to facilitate series connection of PV cells, there is still a path for shunt leakage current that can degrade the fill factor, as illustrated in Fig. 1(b). We examined three approaches to investigate shunt current leakage: 1) semi-insulating substrate alone, 2) p-GaAs junction barrier (500 nm thick, 10^{16} cm^{-3} doping), and 3) p-Al$_{0.3}$Ga$_{0.7}$As junction barrier (400 nm thick, 5×10^{16} cm^{-3} doping). We simulated electrical characteristics for each approach using Synopsys Sentaurus TCAD [15] to obtain optimized parameters for layer thickness, p-type doping concentration, and Al mole fraction. We fabricated PV modules with 8 single PV cells (255 μm x 595 μm) connected in series with 10 μm trenches for device isolation, as shown in Fig. 2. The 8-cell series connection was designed to achieve a voltage output of approximately 5 V for direct battery charging. The PV module design also incorporated a small integrated photodiode for optical communications, and the possibility to incorporate an open location to mount an external sensor (e.g., pressure) for the system. We measured the electrical characteristics of the PV modules under dark and illuminated conditions using Keithley 2400 and 4200 semiconductor characterization tools. Illumination utilized a calibrated white light LED or 850 near-infrared (NIR) LED. The incident LED light intensity was approximately 1 μW/mm^2 (420 lux) to simulate a reasonable indoor or subcutaneous low-flux condition that is approximately 1,000 times smaller than AM 1.5 [16] full sun conditions. We studied incident light dependence by varying the irradiance in increments of 10 lux for white light LED illumination and 100 nW/mm^2 for NIR LED illumination.

3. Results

3.1 Junction barrier isolation
The *J-V* characteristics of fabricated PV modules with p-GaAs and p-Al$_{0.3}$Ga$_{0.7}$As junction barrier isolation are shown in Fig. 3 for 850 nm NIR LED illumination at 1.02 μW/mm^2 and white LED illumination at 586 lux (1.4 μW/mm^2). We extracted diode parameters from single PV cells to simulate the *J-V* characteristics for series-connected cells without shunt leakage, as shown in Fig. 3. PV modules with both p-GaAs and p-Al$_{0.3}$Ga$_{0.7}$As junction barrier isolation produced an open circuit voltage of approximately 5 V. This voltage is near the intended design, and is sufficient for direct battery charging without voltage up-conversion. The PV module with p-GaAs junction barrier isolation demonstrated a dramatic degradation in fill factor from 0.754 to 0.463 in comparison to simulated *J-V* characteristics neglecting the shunt leakage current. As a result, the overall power conversion efficiency under NIR illumination decreases from the expected value of 28.8 % to 15.0 % due to the inability of the GaAs junction barrier to sufficiently block shunt leakage current. We observed a dramatic improvement in performance by incorporating p-Al$_{0.3}$Ga$_{0.7}$As junction barrier isolation, where the measured power conversion efficiency of 26.3

% under NIR illumination compares favorably to the simulated result of 28.8 % for no shunt leakage. The influence of shunt leakage on the performance of monolithic PV modules is further illustrated by the dependence of *J-V* on the number of series-connected cells (p-GaAs junction barrier isolation), as shown in Fig. 4. The overall power conversion efficiency for NIR illumination demonstrates a clear decrease from 21.4 % to 17.5 %, with a fill factor decreasing from 0.71 to 0.582, as the number of series connections increases from 1 to 7. The degradation in the *J-V* characteristics shows an obvious shunt leakage characteristic, as represented by the equivalent circuit model shown in Fig. 1. (c). The *J-V* curves shown in Fig. 3 are representative of our typical module characteristics, where a nonlinear current reduction is observed in the 0-1 V range, followed by an approximately linear shunt resistance current reduction at higher voltages. The nonlinear current reduction at lower voltage may be attributed to non-ideal reverse leakage current through the junction barrier isolation. The characteristics in Fig. 4 demonstrated a more conventional shunt resistance behavior without the nonlinear junction barrier leakage current at low voltage, for which the origin is unclear and is atypical for the majority of samples that we have fabricated. Further discussion of the shunt leakage behavior is described in the following Section 3.2.

3.2 Characteristics of shunt leakage

We measured shunt leakage current between n-contacts of adjacent PV cells without metal interconnects under dark conditions for the three device isolation schemes, as shown in Fig. 5. We observe an approximately linear *I-V* characteristic for the shunt current leakage without junction barrier isolation, suggesting that it is limited by the resistance of the semi-insulating GaAs substrate. We observe a clear reduction in shunt leakage current by incorporating p-GaAs and p-AlGaAs junction barrier isolation. The shunt leakage *I-V* characteristic for the p-GaAs junction barrier has a near exponential dependence, suggesting that leakage is mediated by the energy barrier height of the p-GaAs junction. We observe a further reduction in shunt leakage for the incorporation of a p-AlGaAs junction barrier isolation, which is near the instrument limitation of 1 pA and may be attributed to the increased energy barrier height. The energy barrier height for the three device isolation designs is illustrated in the simulated energy band diagrams shown in Fig. 6. Despite the large reduction in shunt current for the addition of p-GaAs barrier isolation, there is still an obvious degradation in PV module efficiency due to shunt leakage current (Fig. 3). Furthermore, for all three cases of junction barrier isolation, we observe a very low shunt leakage current that is near or below the nA range and would not be expected to dramatically impact PV module efficiency. Therefore, the shunt leakage current characteristics under dark conditions cannot fully explain our observed behavior of the PV modules under illumination.

We subsequently measured the shunt leakage current between n-contacts of adjacent single PV cells under illumination, and observed a substantial increase in leakage current (Fig. 7). The photo-activated behavior may be interpreted as an undesired increase in photoconductivity at the

junction barrier and/or exposed regions of the semi-insulating GaAs substrate. We believe that the nonlinear bias dependence of the photo-activated leakage current may explain the nonlinear shunt leakage current observed in the modules shown in Fig. 3. For all three junction isolation techniques, the shunt current increased by a factor of approximately 100. The shunt leakage for the p-GaAs junction barrier isolation rises to the level of 10 nA, comparable to the photogenerated current, resulting in the observed reduction in PV module performance due to shunt leakage. In contrast, the larger barrier height associated with our p-AlGaAs junction isolation approach significantly improves the ability to block shunt leakage current under illumination. The p-AlGaAs junction barrier isolation limits the shunt leakage current under illumination to approximately 1 nA, preserving the fill factor and overall power conversion efficiency of PV modules.

3.3 Comparison of PV module performance to single PV cell
To gauge the overall power generation of the PV modules, we examined the resulting *P-V* characteristics and compared to a 6.4-mm^2 single PV cell [5], as shown in Fig. 8. The power conversion efficiency of a 1.27-mm^2 PV module with p-AlGaAs junction barrier isolation was 26.3 % under 850 nm infrared LED illumination at 1.02 μW/mm^2 and 16.3 % under white LED indoor conditions at 586 lux (1.4 μW/mm^2). We observed a dramatic decrease in power generation for the p-GaAs junction barrier isolation module, as expected based on the shunt leakage degradation observed in *J-V* characteristics. The power conversion efficiency of the PV module with p-AlGaAs junction barrier isolation, however, approaches the simulated result neglecting shunt leakage current. In comparison to the single PV cell, the PV module with AlGaAs junction barrier isolation provides a voltage that is approximately eight times higher, with approximately 1/8 current reduction. The voltage generated by the PV module is sufficient for direct battery charging, and provides an effective voltage up-conversion efficiency of approximately 90 % for both NIR and white LED illumination.

We observe a strong dependence of power conversion efficiency on incident light intensity, as shown in Fig. 9 for NIR illumination. This dependence has been previously studied for small-area GaAs cells [5], and attributed to perimeter sidewall recombination. Consistent with our *J-V* and *P-V* curves, the shunt leakage current for PV modules with p-GaAs barrier junction isolation results in power conversion efficiency degradation over the full range of light intensity studied. The p-AlGaAs barrier junction isolation module demonstrates power conversion efficiency that approaches the performance of the single PV cell for the full range of illumination intensity. These results confirm that the PV module with p-AlGaAs junction barrier isolation can maintain efficiency comparable to a single PV cell under extremely dim light conditions below 100 nW/mm^2.

3.4 Practical application of mm-scale PV energy harvesting

To illustrate the utility of mm-scale PV modules, we constructed a fully-encapsulated 17 mm^3 wireless sensor system incorporating a GaAs PV module [17] (Fig. 10). The system includes a 16 µAh thin-film lithium-ion battery pair that is directly charged by the PV module through a reverse-current blocking diode. Battery charging characteristics under dim indoor illumination at 110 lux are shown in Fig. 9 (c). The PV module demonstrates a clear recovery of battery voltage within 2 hours, providing adequate energy storage to operate the system. The average power requirement to report temperature every 30 minutes is 28.4 nW, comparing favorably to the average power generation of the PV module of 70.8 nW under 200 lux. While the PV system demonstrates the ability to power a mm-scale wireless sensor nodes, there are still opportunities to further improve conversion efficiency through reducing losses that appear at low light intensity [5] (e.g., perimeter recombination) and losses associated with shunt leakage current for modules [9] providing voltage up-conversion.

4.   Conclusion

Photovoltaic modules offer an efficient means for energy harvesting and direct battery charging in mm-scale systems. This application places unique demands on both PV cells and the module, where PV cells require high performance under much dimmer conditions than conventional solar cells and PV modules have a critical emphasis on maximizing area and electrical isolation of adjacent cells. We demonstrated GaAs PV modules at the mm-scale with high efficiency under low-flux conditions, where AlGaAs junction barrier isolation provided a critical step in limiting shunt leakage current between series connected cells. We observed power conversion efficiency of 26.3 % under 850 nm infrared LED illumination at 1.02 µW/mm^2 and 16.3 % under white LED illumination at 586 lux (1.4 µW/mm^2), with a 90 % voltage up-conversion efficiency to reach an operating voltage of 5 V for direct battery charging. We applied a monolithic PV module to demonstrate the perpetual operation of a mm-scale wirelessly interconnected temperature logger system. Further improvements in mm-scale PV module efficiency may be gained by continued improvement in reducing perimeter leakage current in small-area cells and reduction in shunt leakage through techniques such as epitaxial layer transfer to fully insulating substrates [18] or vertical multi-junction designs [19].

References

[1] Blaauw, D., D. Sylvester, P. Dutta, Y. Lee, I. Lee, S. Bang, Y. Kim et al. "IoT design space challenges: Circuits and systems." In *2014 Symposium on VLSI Technology (VLSI-Technology): Digest of Technical Papers*, pp. 1-2. IEEE, 2014.

[2] Nazari, Meisam Honarvar, Muhammad Mujeeb-U-Rahman, and Axel Scherer. "An implantable continuous glucose monitoring microsystem in 0.18 µm CMOS." In *VLSI Circuits Digest of Technical Papers, 2014 Symposium on*, pp. 1-2. IEEE, 2014.

[3] Moon, Eunseong, David Blaauw, and Jamie D. Phillips. "Subcutaneous photovoltaic infrared energy harvesting for bio-implantable devices." *IEEE transactions on electron devices* 64, no. 5 (2017): 2432-2437.

[4] Teran, Alan S., Eunseong Moon, Wootaek Lim, Gyouho Kim, Inhee Lee, David Blaauw, and Jamie D. Phillips. "Energy harvesting for GaAs photovoltaics under low-flux indoor lighting conditions." *IEEE transactions on electron devices* 63, no. 7 (2016): 2820-2825.

[5] Moon, Eunseong, David Blaauw, and Jamie D. Phillips. "Infrared Energy Harvesting in Millimeter-Scale GaAs Photovoltaics." *IEEE transactions on electron devices* 64, no. 11 (2017): 4554-4560.

[6] Freunek, Monika, Michael Freunek, and Leonhard M. Reindl. "Maximum efficiencies of indoor photovoltaic devices." *IEEE Journal of Photovoltaics* 3, no. 1 (2013): 59-64.

[7] Mathews, Ian, Paul J. King, Frank Stafford, and Ronan Frizzell. "Performance of III–V solar cells as indoor light energy harvesters." *IEEE Journal of Photovoltaics* 6, no. 1 (2016): 230-235.

[8] Martí Vega, Antonio, and Gerardo Lopez Araujo. "Limiting efficiencies of GaAs solar cells." *IEEE Transactions on Electron Devices* 37, no. 5 (1990): 1402-1405.

[9] Kimovec R, Helmers H, Bett AW, Topič M. Comprehensive electrical loss analysis of monolithic interconnected multi   *Prog Photovolt Res Appl 2018;1–11.*

[10] Teran, Alan S., Joeson Wong, Wootaek Lim, Gyouho Kim, Yoonmyoung Lee, David Blaauw, and Jamie D. Phillips. "AlGaAs photovoltaics for indoor energy harvesting in mm-scale wireless sensor nodes." *IEEE Transactions on Electron Devices* 62, no. 7 (2015): 2170-2175.

[11] Moon, Eunseong, David Blaauw, and Jamie D. Phillips. "Small-area Si photovoltaics for low-flux infrared energy harvesting." *IEEE Transactions on Electron Devices* 64, no. 1 (2017): 15-20.

[12] Lee, Inhee, Wootaek Lim, Alan Teran, Jamie Phillips, Dennis Sylvester, and David Blaauw. "A> 78%-efficient light harvester over 100-to-100klux with reconfigurable PV-cell network and MPPT circuit." In *Digest of technical papers/IEEE International Solid-State Circuits Conference. IEEE International Solid-State Circuits Conference*, vol. 2016, p. 370. NIH Public Access, 2016.

[13] Pena, Rafael, and Carlos Algora. "The influence of monolithic series connection on the efficiency of GaAs photovoltaic converters for monochromatic illumination." *IEEE Transactions on Electron*

Devices 48, no. 2 (2001): 196-203.

[14] Takeshiro, Y., Y. Okamoto, and Y. Mita. "Mask-programmable on-chip photovoltaic cell array." In *Journal of Physics: Conference Series*, vol. 1052, no. 1, p. 012144. IOP Publishing, 2018.

[15] Synopsys. *Sentaurus TCAD Version K*   -2015.06.n View, CA: Synopsys Inc.; 2015.

[16] Riordan, C., and R. Hulstron. "What is an air mass 1.5 spectrum?(Solar cell performance calculations)." In *Photovoltaic Specialists Conference, 1990., Conference Record of the Twenty First IEEE*, pp. 1085-1088. IEEE, 1990.

[17] Lee, Inhee, Gyouho Kim, Eunseong Moon, Seokhyeon Jeong, Dongkwun Kim, Jamie Phillips, and David Blaauw. "A 179-Lux Energy-Autonomous Fully-Encapsulated 17-mm 3 Sensor Node with Initial Charge Delay Circuit for Battery Protection." In *2018 IEEE Symposium on VLSI Circuits*, pp. 251-252. IEEE, 2018.

[18] Gai, Boju, Yukun Sun, Haneol Lim, Huandong Chen, Joseph Faucher, Minjoo L. Lee, and Jongseung Yoon. "Multilayer-Grown Ultrathin Nanostructured GaAs Solar Cells as a Cost-Competitive Materials Platform for III–V Photovoltaics." *ACS nano* 11, no. 1 (2017): 992-999.

[19] Datas, A., and P. G. Linares. "Monolithic interconnected modules (MIM) for high irradiance photovoltaic energy conversion: A comprehensive review." *Renewable and Sustainable Energy Reviews* 73 (2017): 477-495.
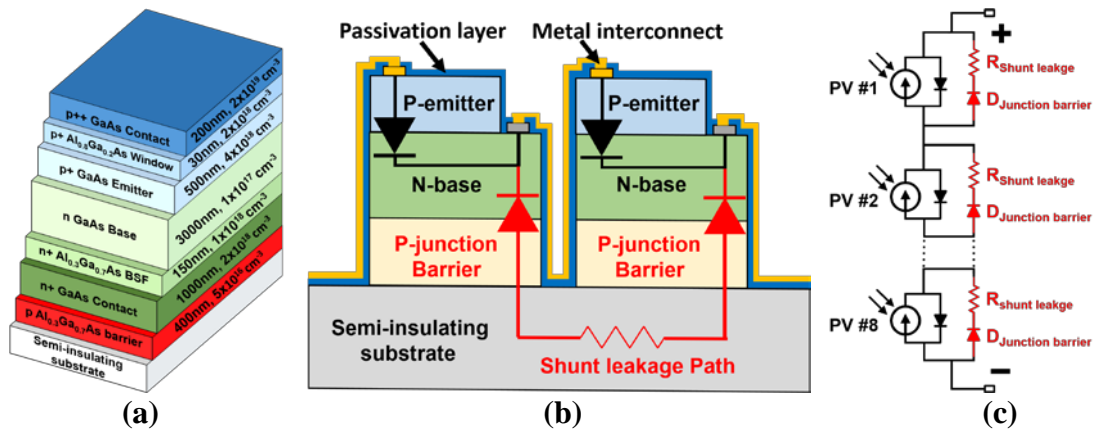
Fig. 1: Schematic diagrams of (a) optimized epitaxial layer structure of a single cell, (b) device structure illustrating PV cell junction, junction barrier isolation, and shunt leakage path, and (c) equivalent circuit model of the PV module.
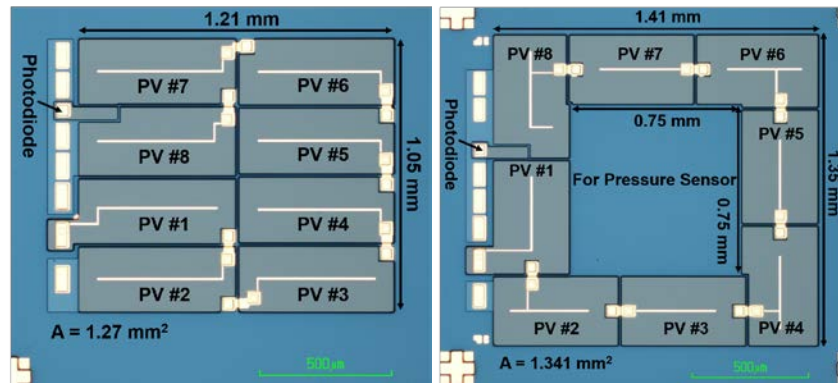
Fig. 2: Optical microscope images of two different fabricated PV modules.
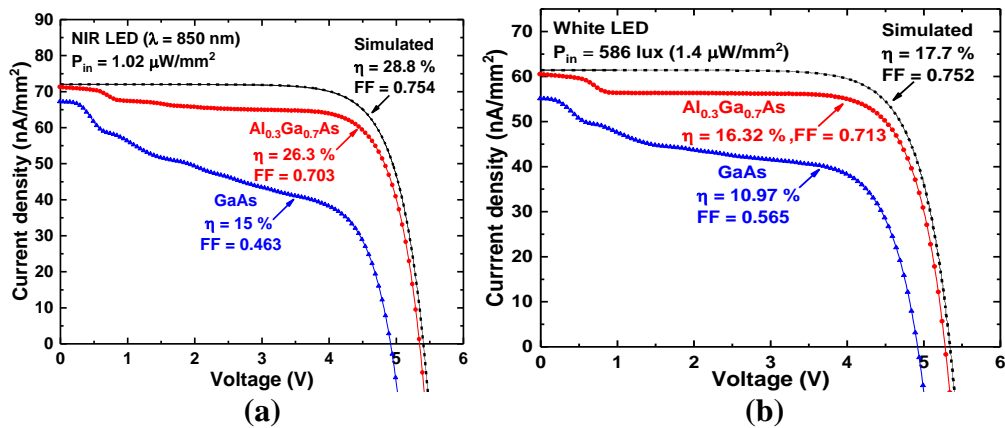
Fig. 3: Measured *J-V* characteristics of PV modules with GaAs and AlGaAs barrier layers (a) under 850 nm NIR LED illumination at 1.02 µW/mm² and (b) under white LED illumination at 586 lux. Comparisons are shown to simulated results (dashed) with shunt leakage removed.
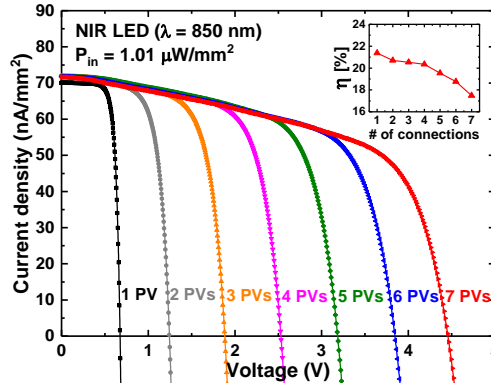
Fig. 4: Measured *J-V* curves for varying number of PV cell series connection and (inset) corresponding power conversion efficiency at the maximum power point.
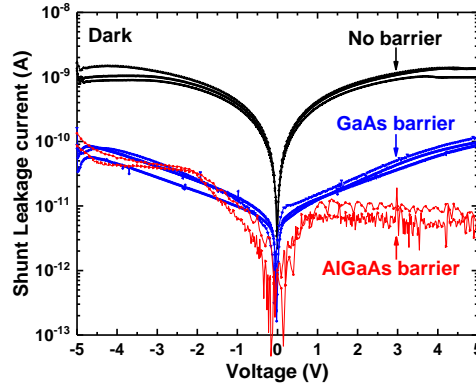
Fig. 5: Measured shunt leakage current under dark conditions for three different barrier structures: no barrier, p-GaAs junction, and p-Al$_{0.3}$Ga$_{0.7}$As junction.
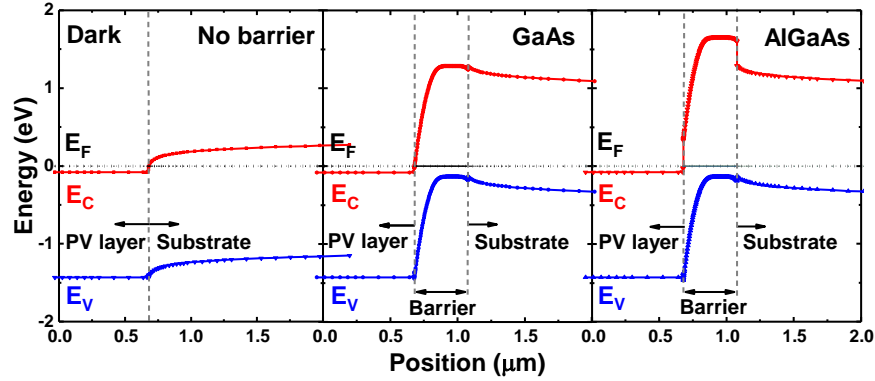
Fig. 6: Simulated energy band diagrams between the PV cell base and semi-insulating substrate under dark conditions for three different barrier layer structures: no barrier, p-GaAs junction, and p-Al$_{0.3}$Ga$_{0.7}$As junction.
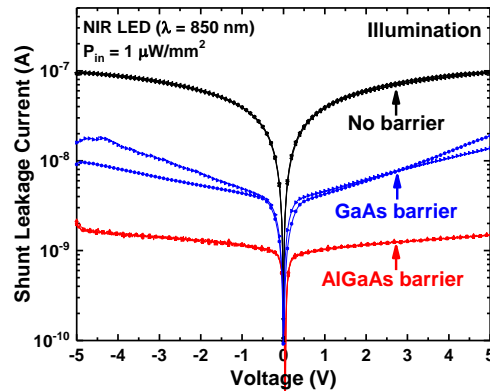
Fig 7: Measured shunt leakage current under NIR LED illumination for three different barrier structures: no barrier, p-GaAs junction, and p-Al$_{0.3}$Ga$_{0.7}$As junction.
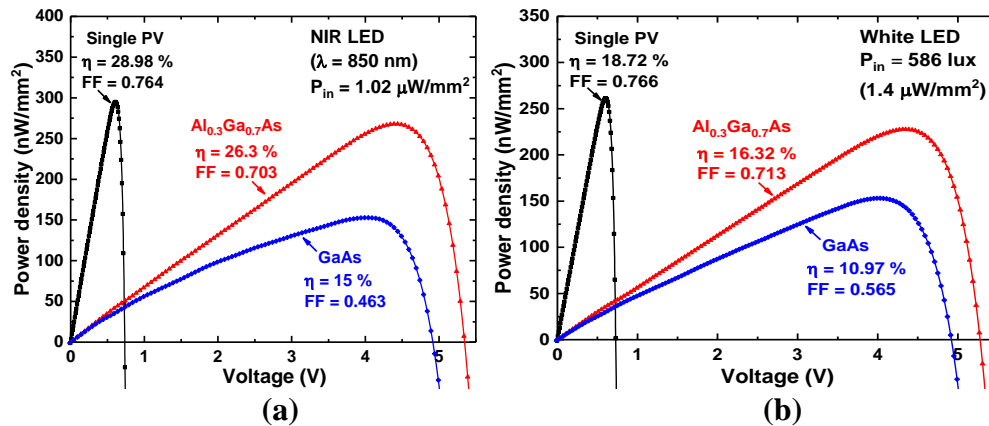
Fig. 8: Comparison of measured *P-V* characteristics between PV arrays and single PV cell (a) under 850 nm NIR illumination at 1.02 µW/mm^2 and (b) under white LED illumination at 586 lux.
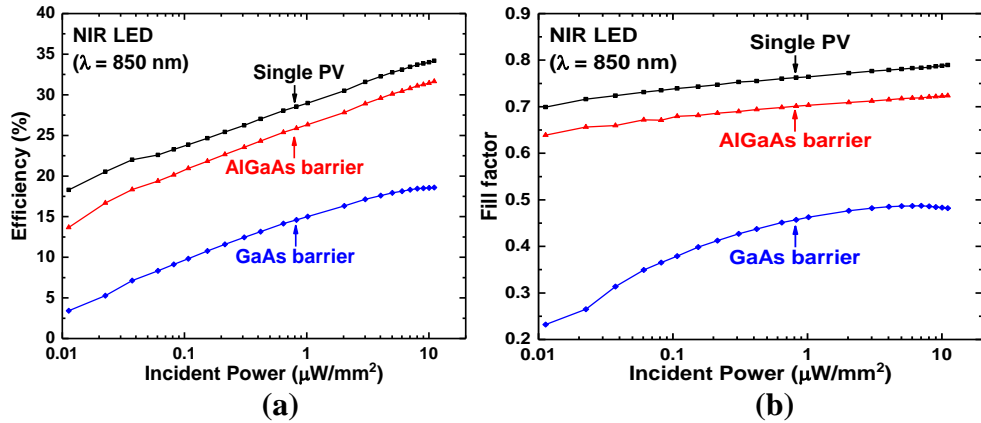
Fig. 9: Light intensity dependence of (a) power conversion efficiency and (b) fill factor for single PV and PV modules with p-GaAs and p-AlGaAs barrier junction isolation.
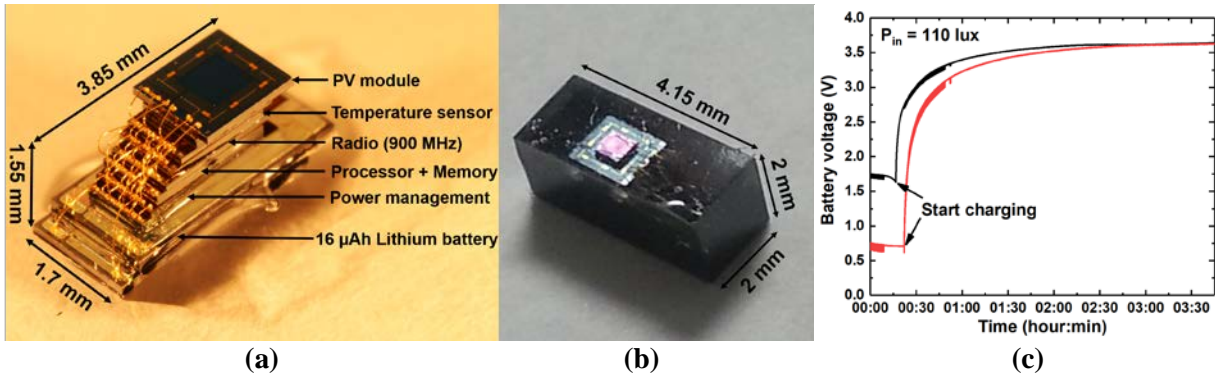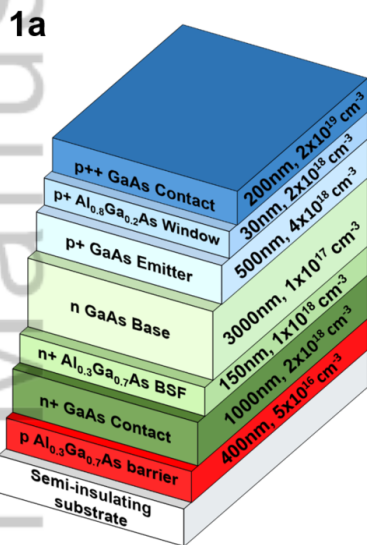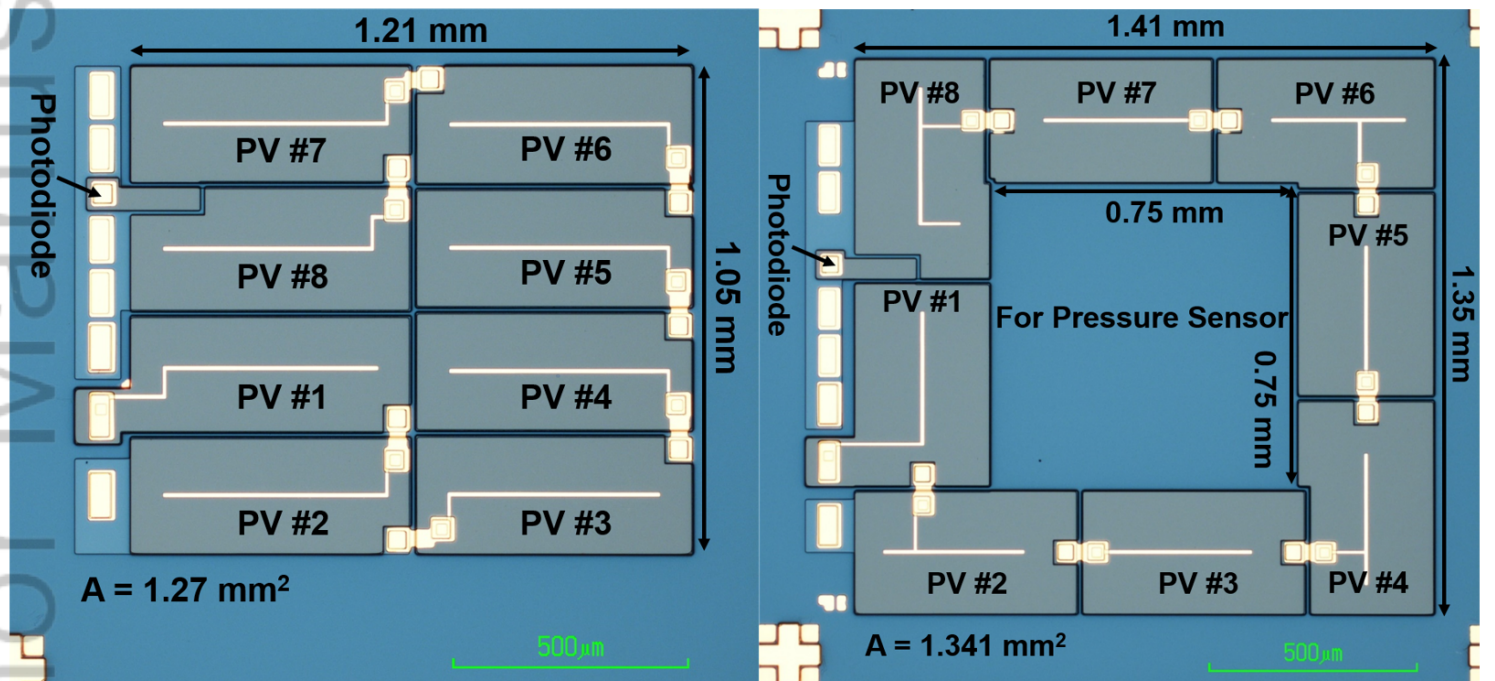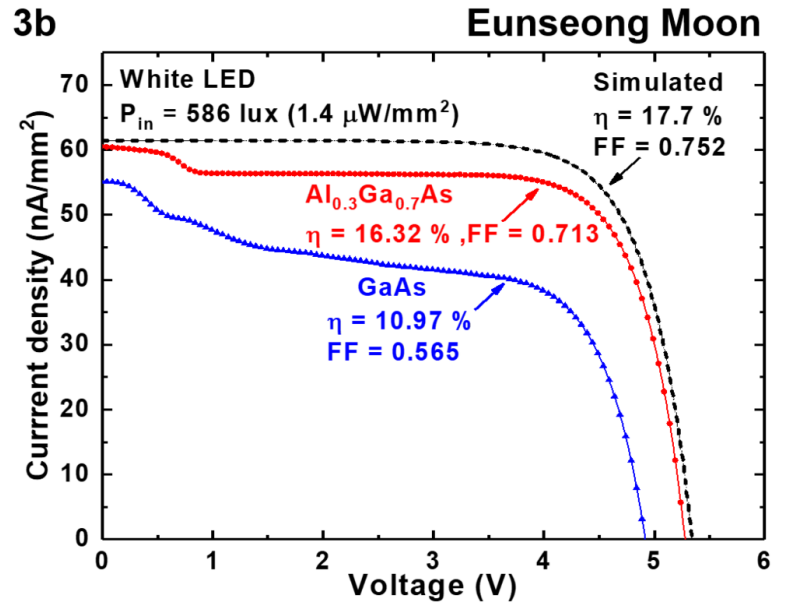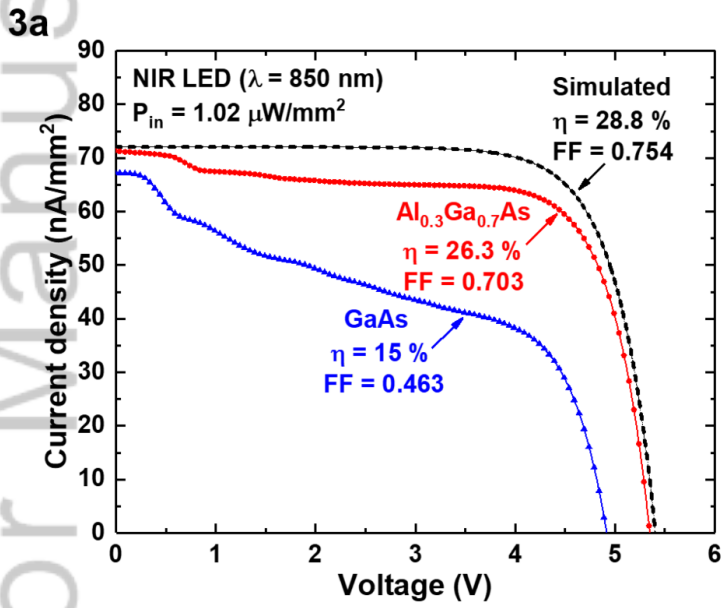

Fig. 10: Optical microscope images of a wireless mm-scale sensor system with integrated PV module (a) before and (b) after encapsulation. (c) Monitored battery voltage output of this mm-scale system during the charging process under 110 lux indoor illumination.
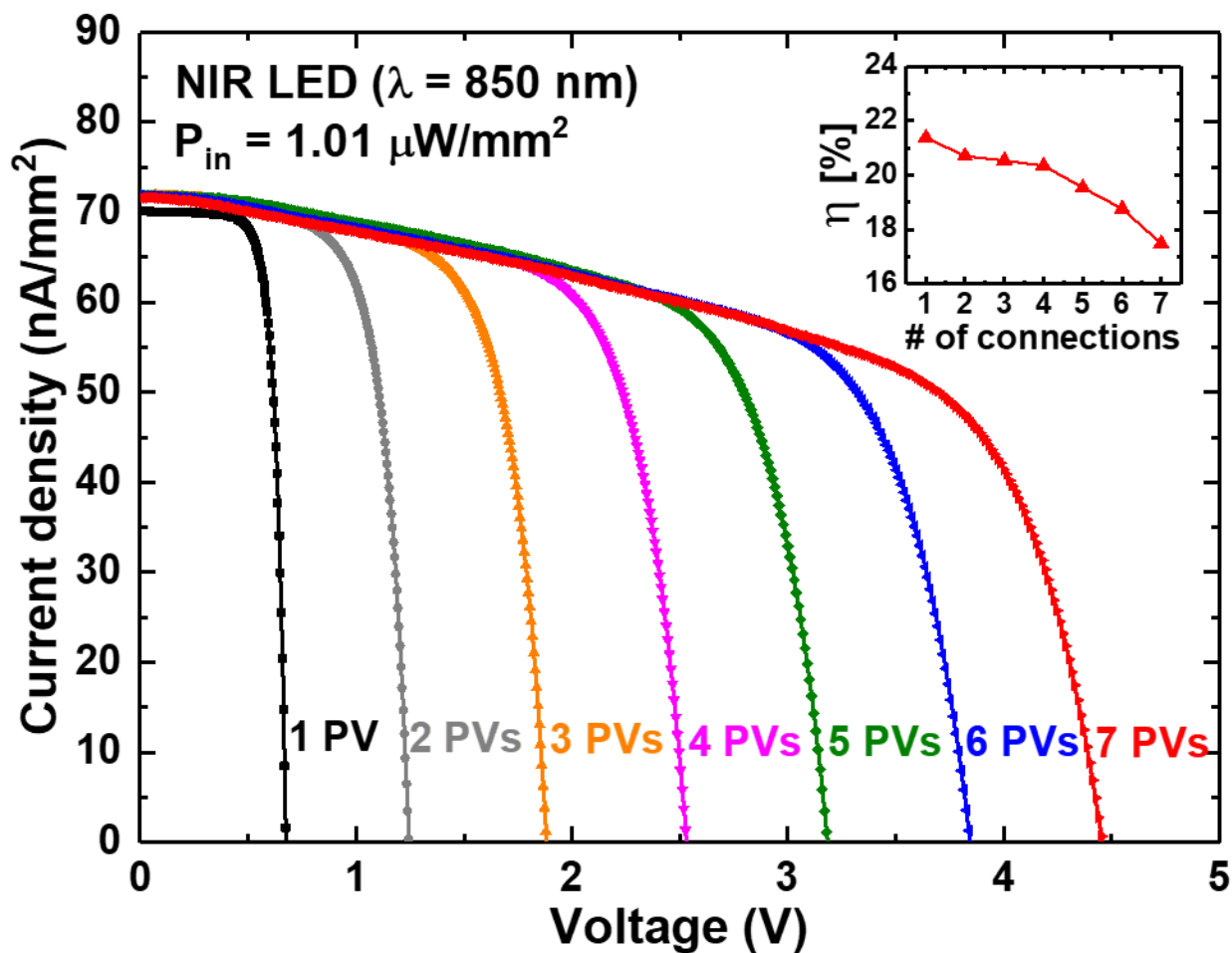
1a

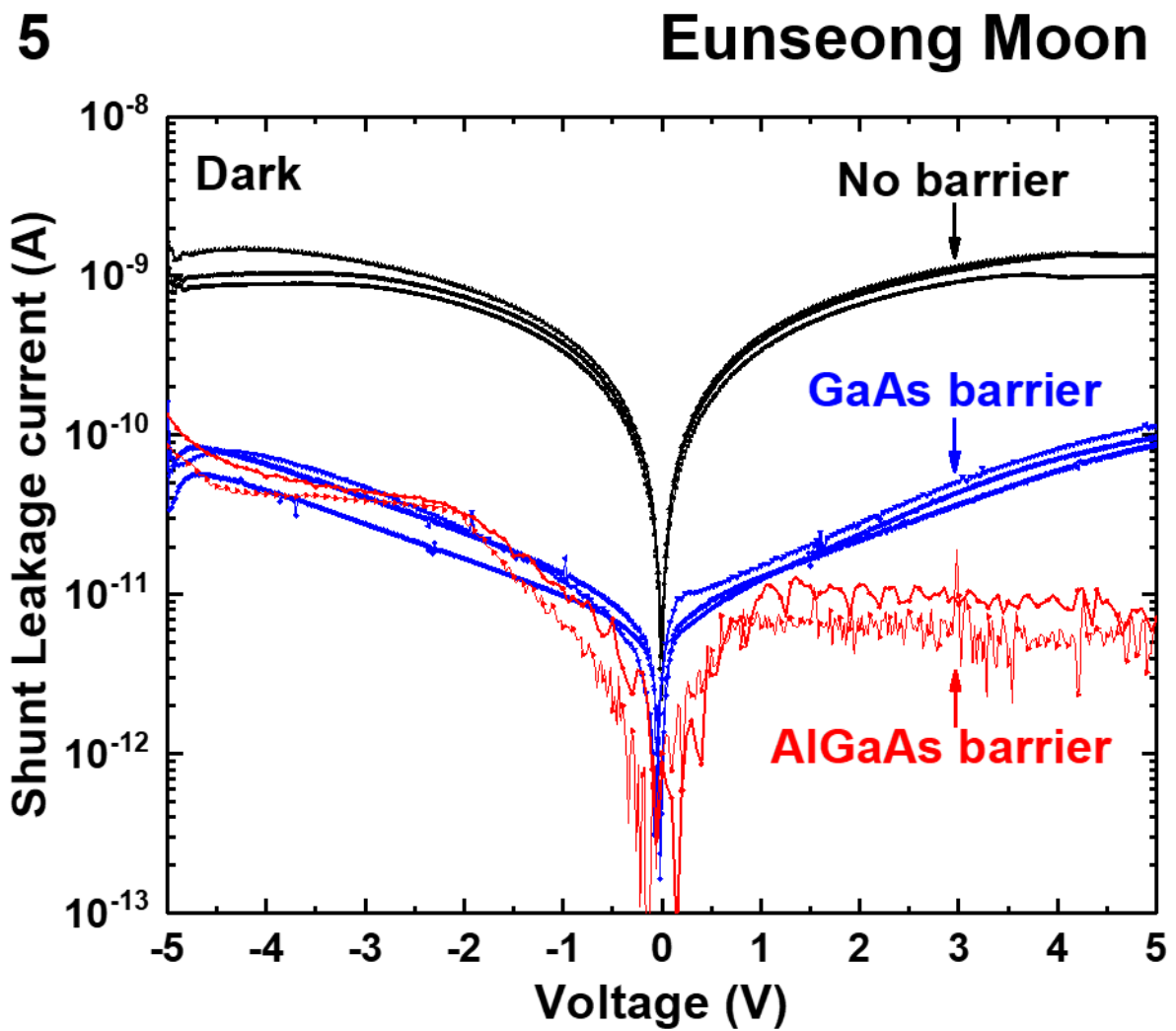200nm, 2x10^{19} cm^{-3} — p++ GaAs Contact
30nm, 2x10^{18} cm^{-3} — p+ Al$_{0.8}$Ga$_{0.2}$As Window
500nm, 4x10^{18} cm^{-3} — p+ GaAs Emitter
3000nm, 1x10^{17} cm^{-3} — n GaAs Base
150nm, 1x10^{18} cm^{-3} — n+ Al$_{0.3}$Ga$_{0.7}$As BSF
1000nm, 2x10^{18} cm^{-3} — n+ GaAs Contact
400nm, 5x10^{16} cm^{-3} — p Al$_{0.3}$Ga$_{0.7}$As barrier
Semi-insulating substrate

1b

Passivation layer   Metal interconnect

P-emitter

N-base

P-junction Barrier

Semi-insulating substrate

Shunt leakage Path

1c

PV #1   R$_{Shunt\ leakge}$ D$_{Junction\ barrier}$

PV #2   R$_{Shunt\ leakge}$ D$_{Junction\ barrier}$

PV #8   R$_{shunt\ leakge}$ D$_{Junction\ barrier}$

Eunseong Moon

PIP_3132_F1.tif

PIP_3132_F2.tif

3a

NIR LED (λ = 850 nm)
P_{in} = 1.02 μW/mm^2

Simulated
η = 28.8 %
FF = 0.754

Al$_{0.3}$Ga$_{0.7}$As
η = 26.3 %
FF = 0.703

GaAs
η = 15 %
FF = 0.463

Current density (nA/mm^2)

Voltage (V)

3b   **Eunseong Moon**

White LED
P_{in} = 586 lux (1.4 μW/mm^2)

Simulated
η = 17.7 %
FF = 0.752

Al$_{0.3}$Ga$_{0.7}$As
η = 16.32 % ,FF = 0.713

GaAs
η = 10.97 %
FF = 0.565

Currrent density (nA/mm^2)

Voltage (V)

PIP_3132_F3.tif

PIP_3132_F4.tif

PIP_3132_F5.tif

Eunseong Moon
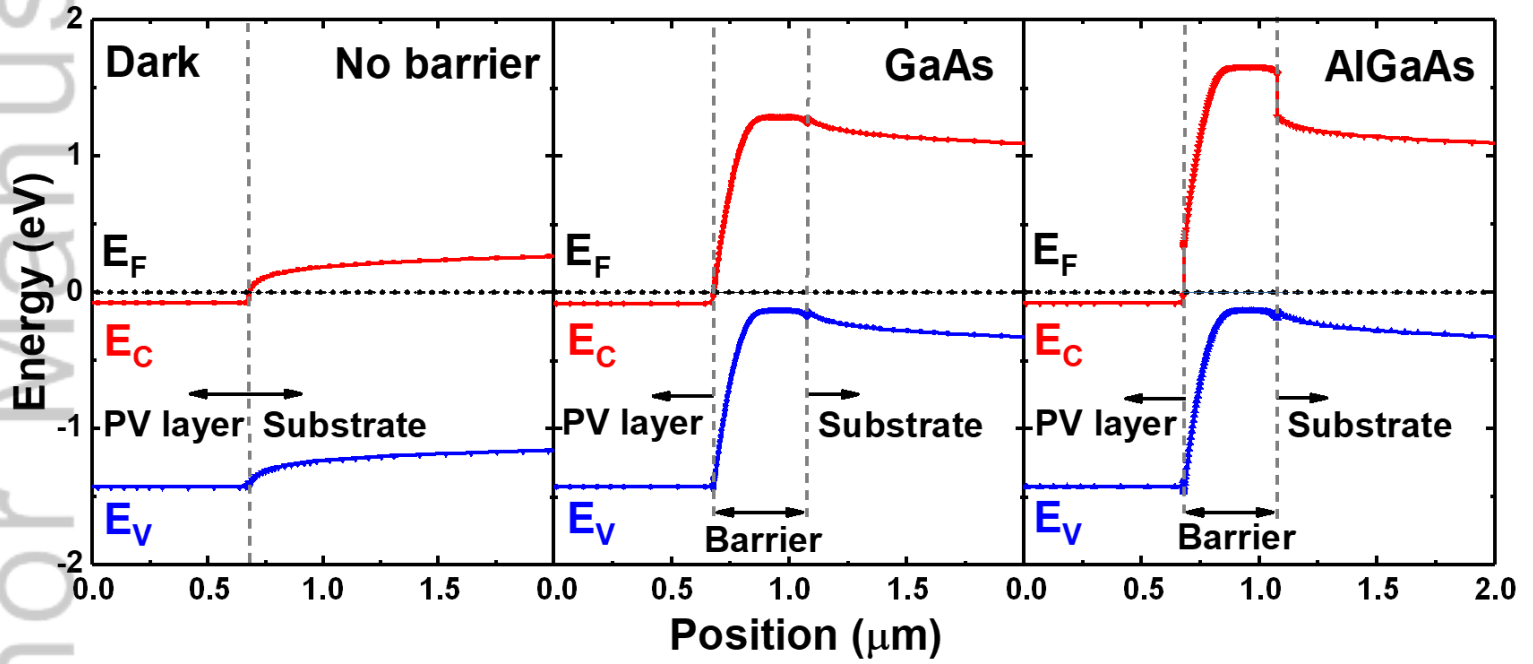
PIP_3132_F6.tif

PIP_3132_F7.tif

8a — Single PV: η = 28.98 %, FF = 0.764; NIR LED (λ = 850 nm), P_in = 1.02 μW/mm². Al₀.₃Ga₀.₇As: η = 26.3 %, FF = 0.703. GaAs: η = 15 %, FF = 0.463.

8b — Single PV: η = 18.72 %, FF = 0.766; White LED, P_in = 586 lux (1.4 μW/mm²). Al₀.₃Ga₀.₇As: η = 16.32 %, FF = 0.713. GaAs: η = 10.97 %, FF = 0.565.

PIP_3132_F8.tif

9a

9b   **Eunseong Moon**

PIP_3132_F9.tif

10a

- PV module
- Temperature sensor
- Radio (900 MHz)
- Processor + Memory
- Power management
- 16 µAh Lithium battery

3.85 mm
1.55 mm
1.7 mm

10b

4.15 mm
2 mm
2 mm
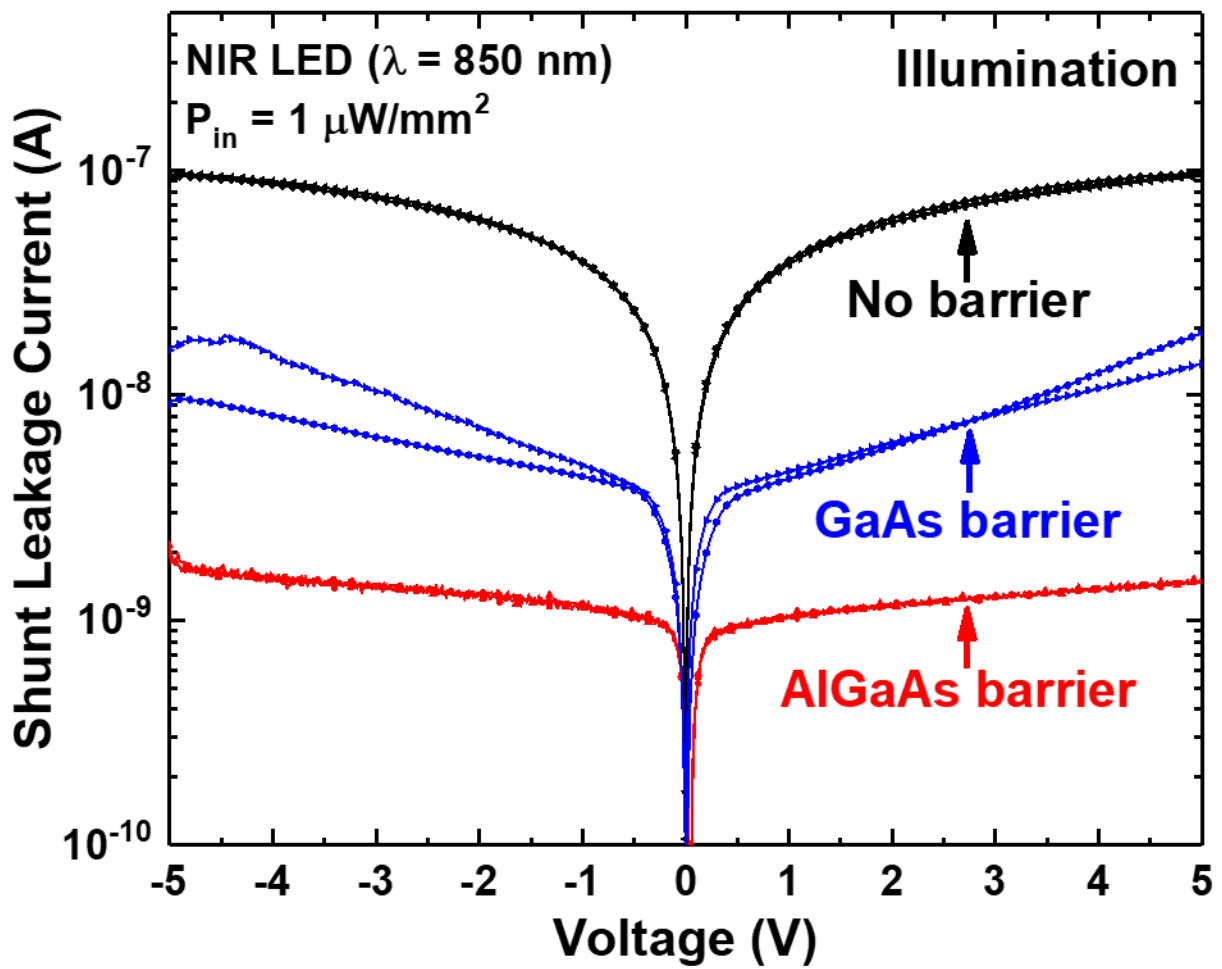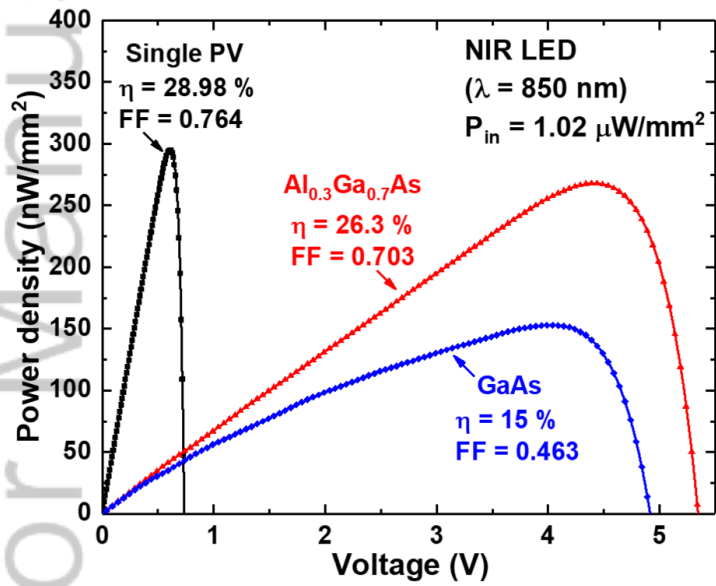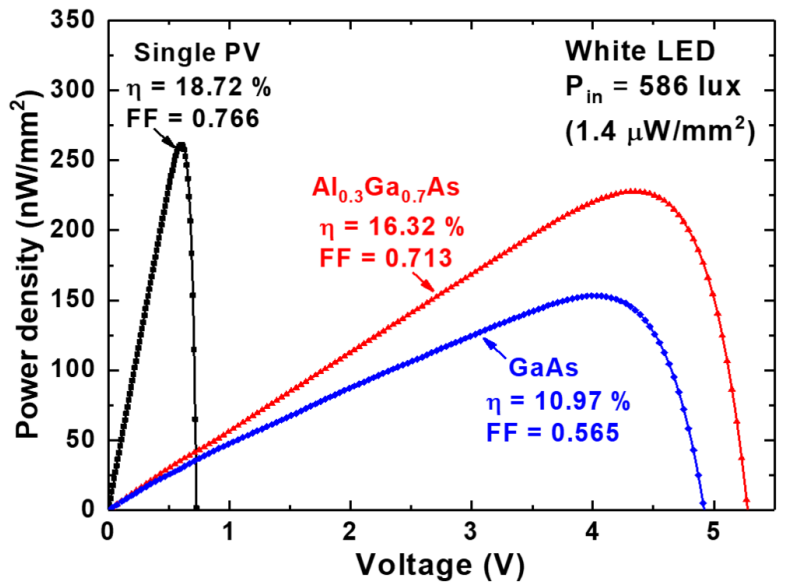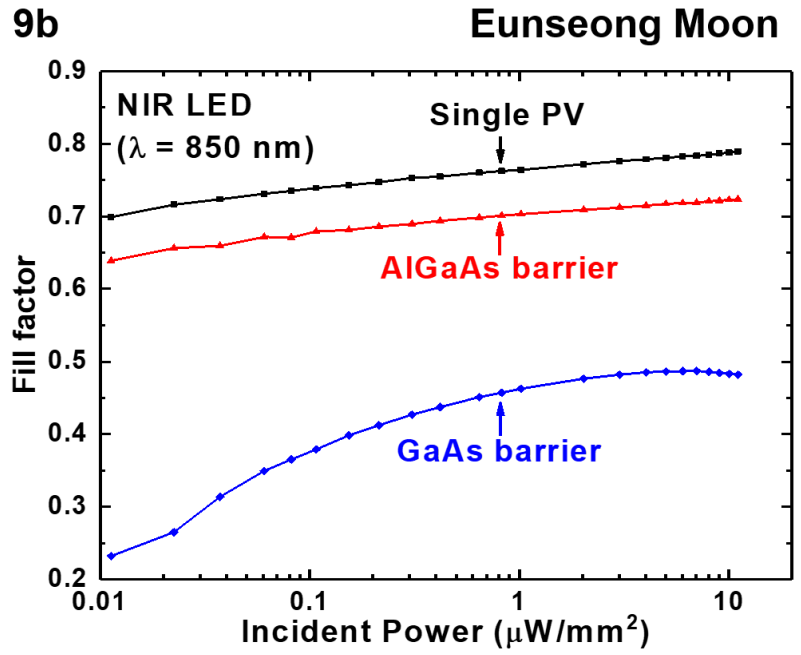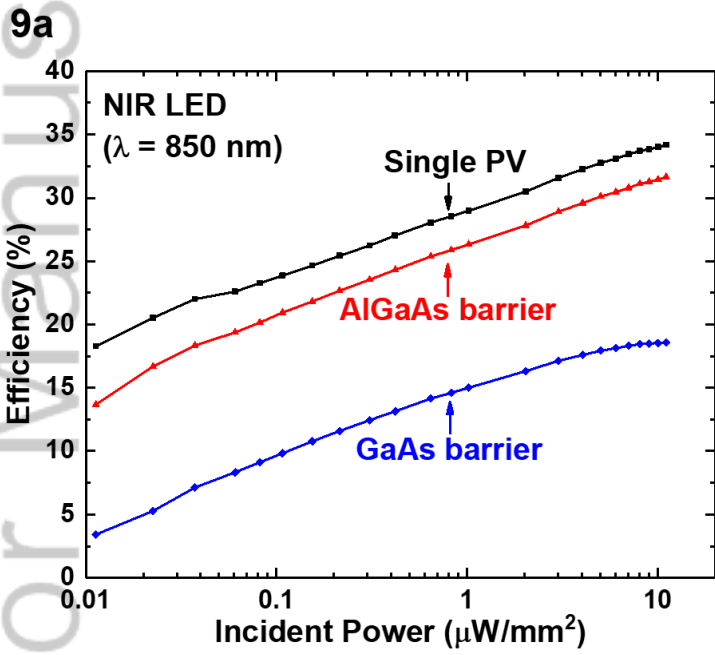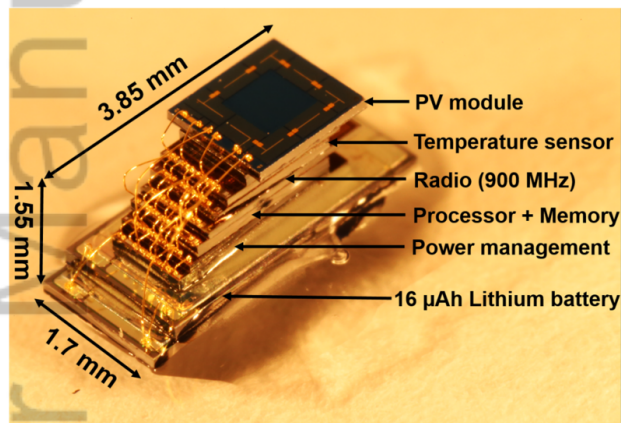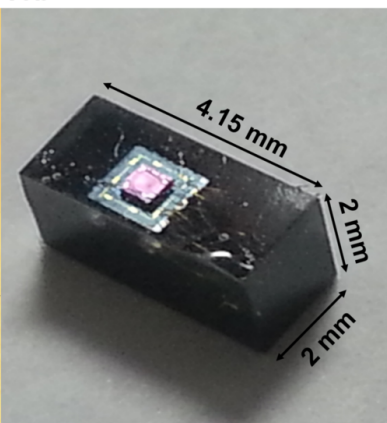
PIP_3132_F10.tif

10c **Eunseong Moon**
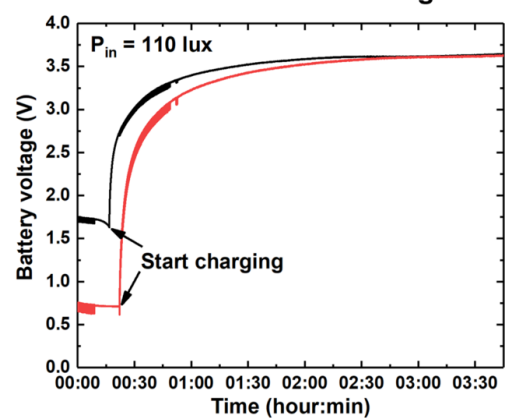
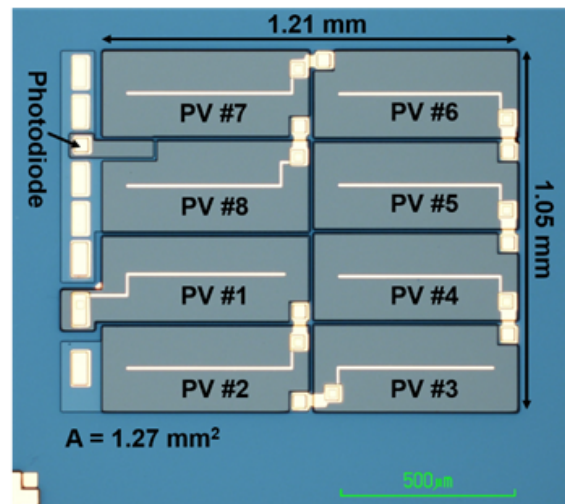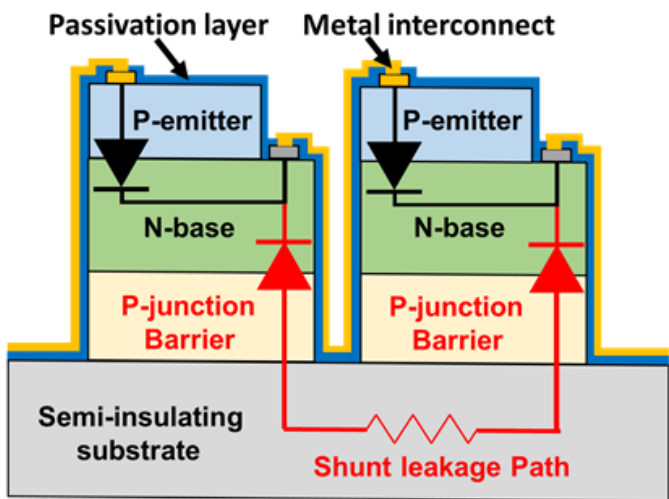P_{in} = 110 lux

Start charging

Battery voltage (V)

Time (hour:min)

High-Efficiency Photovoltaic Modules on a Chip
for Millimeter-Scale Energy Harvesting

Eunseong Moon, Inhee Lee, David Blaauw and Jamie D. Phillips*

We demonstrate monolithic GaAs photovoltaic modules at the mm-scale to efficiently power wirelessly interconnected mm-scale sensor systems operating under low-flux conditions. Eight series-connected cells are used to provide an operating voltage of 5 V for direct battery charging. Module power conversion efficiency greater than 26 % is achieved under weak 850 nm near infrared illumination and 90 % voltage up-conversion efficiency utilizing AlGaAs junction barrier isolation as a critical technique in reducing shunt leakage current.

PIP_3132_GTOC.tif